International Journal of
Molecular Sciences

MDPI

Article

Sex-Divergent Patterns in Hippocampal and Cortical NMDA Receptor Density Across the Alzheimer's Disease Continuum

Maricedes Acosta-Martínez [1,*], Vanessa Carter [2], Aviram Nessim [1], Sarah Murphy [1], Jasbeer Dhawan [2], Thomas G. Beach [3], Geidy E. Serrano [3], Erin E. Sundermann [4] and Anat Biegon [2]

1 Department of Physiology and Biophysics, Renaissance School of Medicine at Stony Brook University, Stony Brook, NY 11794, USA; avinessim@gmail.com (A.N.); sarah.murphy.2@stonybrook.edu (S.M.)
2 Department of Radiology, Renaissance School of Medicine at Stony Brook University, Stony Brook, NY 11794, USA; vcarter612@gmail.com (V.C.); jasbeerdhawan@gmail.com (J.D.); anat.biegon@stonybrook.edu (A.B.)
3 Banner Sun Health Research Institute, Sun City, AZ 85351, USA; thomas.beach@bannerhealth.com (T.G.B.); geidy.serrano@bannerhealth.com (G.E.S.)
4 Department of Psychiatry, University of California, San Diego, CA 92093, USA; esundermann@health.ucsd.edu
* Correspondence: maricedes.acosta@stonybrook.edu; Tel.: +1-631-444-6075

Abstract

While the loss of NMDA receptors (NMDARs) is associated with Alzheimer's disease (AD) severity, the effect of sex or the relationship between regional NMDAR density and antemortem cognitive status across the AD spectrum has not been examined. We performed quantitative in vitro autoradiography of the hippocampus, entorhinal cortex (EC), and parietal cortex using NMDAR and tau radioligands. Relationships between regional NMDAR density and cognitive status assessed by the Mini Mental State Examination (MMSE), and between NMDAR and tau density, were examined by bivariate correlations. In both sexes, the largest AD-related decreases in NMDAR density were observed in the cornu ammonis 1 (CA1) field. However, there was a significant diagnosis by sex interaction driven by sex-specific differences in the mild cognitive impairment (MCI) stage, with lower NMDAR density in MCI women, but not MCI men relative to same-sex controls. Within diagnosis analyses revealed positive correlations between NMDAR density and MMSE scores and significant negative correlations between EC NMDAR and tau density, which was significant only in AD men. Our data show that differences in hippocampal NMDAR density across the AD continuum are modulated by sex and may contribute to the known sex differences in the clinical trajectory of the disease.

Keywords: sex; NMDA receptors; hippocampus; parietal cortex; entorhinal cortex; tau; MMSE

Academic Editor: Natalia V. Gulyaeva

Received: 26 July 2026
Revised: 20 September 2026
Accepted: 22 September 2026
Published: 25 September 2026

Copyright: © 2026 by the authors. Licensee MDPI, Basel, Switzerland. This article is an open access article distributed under the terms and conditions of the Creative Commons Attribution (CC BY) license.

1. Introduction

Alzheimer's disease (AD) is a progressive neurodegenerative disorder characterized by the deposition of amyloid plaques and tau-containing neurofibrillary tangles. Clinically, the hallmark of AD is cognitive decline, and the glutamatergic system, specifically the NMDA receptor (N-methyl-D-aspartate receptor, NMDAR), plays a major role in cognitive processes [1,2]. NMDARs, which are essential for synaptic plasticity and memory formation, are highly concentrated in the human hippocampus [3,4]. As such,

the loss of functional NMDAR and the resulting impairment in NMDA-evoked Long-Term Potentiation (LTP) is a central mechanism in AD that links the initial memory loss with the characteristic neurodegeneration of the hippocampus [5–7].

Studies in humans and in animal models have described multiple interactions between amyloid beta, phosphorylated tau and various glutamatergic transmission markers, underscoring the importance and complexity of the role played by NMDAR in AD [8–19]. Early work indicated the loss of NMDAR, as measured by autoradiography, in the postmortem cortex and hippocampus of AD patients [20–22]. This was confirmed by our own autoradiographic study [23] demonstrating AD-related decreases in NMDAR density in the hippocampus and entorhinal cortex (EC), which tracks with disease severity as assessed by Braak staging. Conversely, several studies using different techniques found evidence for increased NMDAR protein and activation in early AD [16,24,25]. The reasons behind the inconsistent results are unknown, however, the above-mentioned studies did not examine the effects of sex or the relationship between regional NMDAR density and antemortem cognitive status across the AD spectrum. This is an important gap in the field since sex differences in hippocampal expression of NMDARs may contribute to the known sex differences in the cognitive trajectory of the disease, characterized by a female cognitive advantage in early disease stages followed by accelerated decline once pathology surpasses a critical threshold [26,27].

Utilizing in vitro autoradiography with the specific NMDAR antagonist [^{3}H]-MK801, we performed the first fully quantitative analysis of NMDAR density in the hippocampal formation, EC, and parietal cortex (PC) of women and men who died with a clinical diagnosis of AD dementia, Mild Cognitive Impairment (MCI, the prodromal stage of AD), or cognitively normal (CN) controls. Given the well-documented selective vulnerability of the CA1 subfield to neurodegeneration in AD, driven in part by its direct monosynaptic input from the EC and consequent EC-tau-related deafferentation [28–33], we hypothesize that AD-related reductions in NMDAR density would be most pronounced in the CA1. Furthermore, we examined the relationship between regional NMDAR density and antemortem cognitive function assessed by the Mini-Mental State Examination test (MMSE), and between NMDAR and tau density in women and men across the AD continuum.

2. Results

2.1. Sample Characteristics

The characteristics of men and women in each diagnostic group are summarized in Table 1. There were no significant main effects of diagnosis, sex, or their interaction on postmortem delay or years of education (two-way ANOVAs, all $p > 0.05$). For age, a two-way ANOVA revealed a significant main effect of diagnosis ($p = 0.0005$), with no significant effect of sex ($p = 0.91$) or diagnosis × sex interaction ($p = 0.995$). Thus, the MCI group showed the highest mean age in both sexes (Table 1), although pairwise post-hoc comparisons did not reach significance. Within the AD group specifically, ApoE4 allele carriership was more frequent in men with AD compared to men in the CN and MCI groups ($p < 0.01$, Fisher's exact test); while in women, ApoE4 carriership frequency did not differ significantly across the CN, MCI, and AD diagnostic groups.

Table 1. Characteristics of tissue donors by sex.

Characteristics	Women (*n* = 76)			Men (*n* = 79)		
	CN (*n* = 25)	MCI (*n* = 24)	AD (*n* = 26)	CN (*n* = 26)	MCI (*n* = 26)	AD (*n* = 27)
Age years (SD)	83.1 (12.0)	89.0 (6.6)	83.3 (11.1)	82.8 (7.2)	89.0 (6.4)	83.0 (7.1)
Education (SD)	14.6 (2.6)	14.9 (3.1)	14.1 (2.7)	15.3 (3.3)	14.5 (2.6)	14.7 (3.2)
Non-Hispanic white, n (%)	25 (100)	23 (100) [a]	24 (92)	24(100) [b]	26 (100)	25 (100)
APOE e4 carriers, n (%)	5 (20)	5 (21)	6 (24) [a]	4 (15)	8 (31)	16 (59)
PMI hours (SD)	3.6 (1.3)	4.3 (2.4)	3.3 (1.0)	4.6 (2.3)	4.0 (1.3)	3.6 (1.5)
Global Cognition (MMSE)	28.2 (1.8)	25.4 (3.1) **	14.6 (7.6) **	27.9 (2.0)	24.9 (2.7) **	14.6 (8.7) **

There were no sex differences in age, years of education, PMI, MMSE scores (ANOVA, $p > 0.05$) or in APOE ε4 carrier frequency (Fisher's exact test, $p = 0.074$). [a,] Information unavailable from one subject. [b,] Information unavailable from two subjects. MMSE scores differed significantly by diagnosis (two-way ANOVA, $p < 0.001$). ** Significantly different from the other diagnostic groups (Bonferroni-adjusted post hoc comparisons, all $p < 0.001$). CN = cognitively normal; MCI = mild cognitive impairment; AD = Alzheimer's disease; PMI = postmortem interval; MMSE = Mini-Mental State Examination. Values are *n* (%) or mean (SD) unless otherwise indicated.

As expected, MMSE scores differed significantly by diagnosis (two-way ANOVA, $p < 0.001$). Bonferroni-adjusted post hoc comparisons showed significant differences between CN, MCI, and AD groups (all $p < 0.001$). However, no significant main effect of sex or a sex by diagnosis interaction was observed ($p > 0.05$).

2.2. The Effect of Diagnosis on NMDA Receptor Density Is Modulated by Sex

The anatomical distribution of NMDARs in the hippocampus and cortex of CN individuals was similar to the known distribution of NMDARs in the human brain (Figure 1, [23]), with the highest densities in the CA1 (women: 10.8 ± 0.6; men: 9.8 ± 0.6) and dentate gyrus (DG; women: 10.8 ± 0.5; men: 9.6 ± 0.4) and the lowest densities in cortical white matter (women: 1.0 ± 0.51; men: 0.15 ± 0.08).

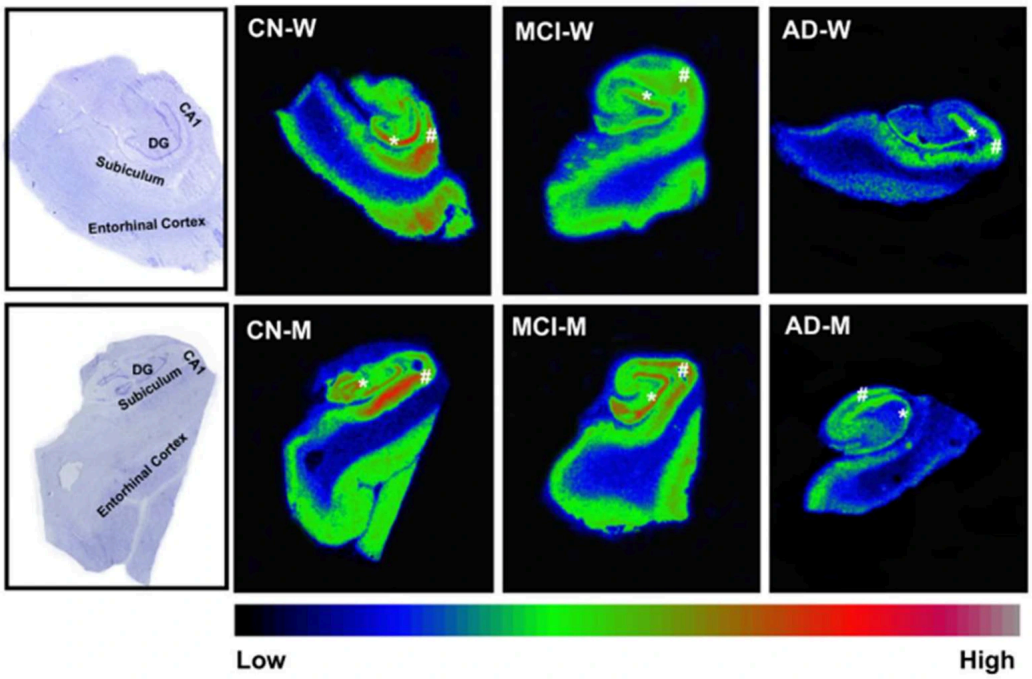


Figure 1. NMDA receptor density in the hippocampus and adjacent entorhinal cortex of women and men with antemortem clinical diagnosis of cognitively normal (CN), mild cognitive impair-

ment (MCI), and Alzheimer's disease (AD) dementia measured with [^{3}H]-MK801 autoradiography. Verification of anatomy is illustrated in the leftmost panel, showing histological (cresyl violet) staining of consecutive sections from adjacent CN subjects, followed by representative pseudo-colored autoradiograms of NMDA receptor binding labeled with [^{3}H]-MK801 from the hippocampus and EC of CN, MCI, and AD women (top) and men (bottom). Autoradiograms were pseudo-colored using the Rainbow RGB lookup table (bottom bar); asterisks point to the DG, hash point to the CA1. Note highest NMDA receptor density observed in the CA1 and DG of CN subjects. Abbreviations: W, Woman; M, Man; CA1 = cornu ammonis field 1 of the hippocampus; DG, dentate gyrus; CN, cognitively normal; MCI, mild cognitive impairment; AD, Alzheimer's disease.

A three-way ANCOVA (factors: region, diagnosis, and sex) of NMDAR density, with age and years of education as covariates, showed a significant effect of region ($p < 0.001$; DG > CA1 > subiculum (S) > EC > PC), a significant main effect of diagnosis ($p = 0.045$), and a highly significant sex × diagnosis interaction ($p = 0.007$). There was no significant main effect of sex ($p = 0.447$), no significant sex × region interaction ($p = 0.838$), no significant region × diagnosis interaction ($p = 0.240$), and no significant sex × region × diagnosis interaction ($p = 0.968$). Moreover, the covariates age ($p = 0.950$) and years of education ($p = 0.838$) did not have a statistically significant effect on NMDAR density; the three-way ANCOVA was therefore re-run as a three-way ANOVA without covariates and yielded the same pattern of significant effects.

To probe the significant sex × diagnosis interaction, we performed sex-stratified 2-way ANOVAs with region and diagnosis as fixed factors. A significant main effect of region and diagnosis on NMDAR density was observed in both sexes (region, $p < 0.01$; diagnosis, women, $p = 0.01$; men, $p = 0.03$); however, a sex-specific pattern in the diagnosis effect emerged, whereby women showed a lower NMDAR density in both MCI and AD groups relative to CN (Figure 2A), whereas men showed a lower NMDAR density only in the AD group relative to the MCI and CN groups (Figure 2B). As hypothesized, this pattern reached statistical significance most prominently in the CA1 field of both men and women, a region of known vulnerability [28–33] (Figure 2A,B; women: AD < CN, $p < 0.05$; MCI < CN, $p = 0.06$, MCI = AD; men: MCI > AD, $p < 0.05$; CN > AD, $p = 0.06$, CN = MCI).

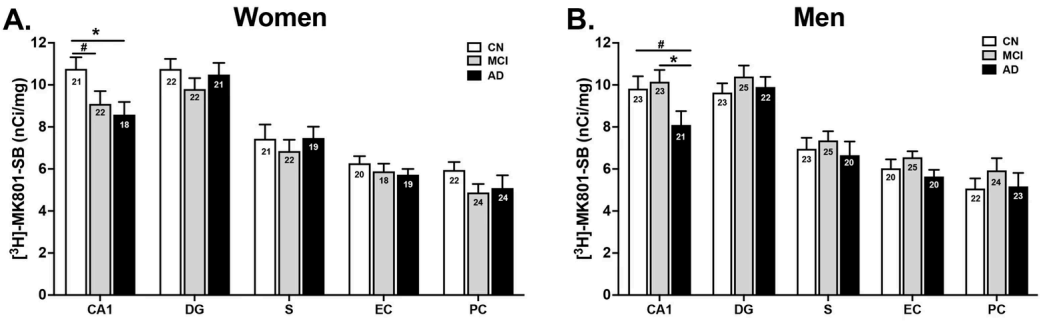


Figure 2. Diagnosis effects on NMDA receptor densities across hippocampal subregions and cortical regions are modulated by sex. Results of quantitative autoradiographic measurements of regional NMDA receptor density (expressed as specific binding of [^{3}H]-MK801 in nCi/mg tissue) across diagnosis in women (**A**), and men (**B**). * $p < 0.05$, AD relative to CN in women or relative to MCI in men; #, approaching significance, $p = 0.06$. Results are from 2-way ANOVAs following a significant sex by diagnosis interaction ($p < 0.01$) in a 3-way ANCOVA with age and years of education as covariates. Bonferroni adjustment was used for correction. Note a similar pattern of a reduction in NMDA receptor density in both MCI and AD women relative to CN controls across regions, whereas in men NMDAR densities in MCI are maintained at levels that are not significantly different from CN controls. Data are presented as mean ± SEM. Numbers inside bars denote the

number of subjects with useful data per region and diagnosis. Abbreviations: CA1, cornu ammonis field 1 of the hippocampus; DG, dentate gyrus; S, subiculum; EC = entorhinal cortex; PC, parietal cortex; SB, specific binding; CN, cognitively normal; MCI, mild cognitive impairment; AD, Alzheimer's disease.

To account for within-donor dependence among regional measurements, we additionally performed a linear mixed-model sensitivity analysis in which region was modeled as a repeated factor within donor using a compound-symmetry covariance structure and Satterthwaite degrees of freedom. The main effect of region remained significant ($p < 0.001$), whereas the sex × diagnosis ($p = 0.104$), diagnosis × region ($p = 0.074$), and sex × diagnosis × region ($p = 0.955$) interactions were not significant. Follow-up simple-effects analyses showed a significant effect of diagnosis in CA1 in both women ($p = 0.008$) and men ($p = 0.032$), whereas diagnosis effects were not significant in the other regions. Bonferroni-adjusted comparisons showed that, in women, CA1 NMDAR density was lower in both MCI ($p = 0.050$) and AD ($p = 0.010$) relative to CN controls, whereas in men, CA1 NMDAR density was significantly higher in MCI than in AD ($p = 0.043$).

2.3. The Relationship Between NMDA Receptor Density and Cognitive Scores Is Positive and Significant in Men but Not Women with Alzheimer's Disease

Next, we examined the relationship between NMDAR density in the CA1 and cognitive status as measured by the MMSE. Across sexes and diagnostic groups, we found a significant positive correlation between NMDAR density in the CA1 and MMSE scores ($n = 124$, r = 0.24, $p < 0.01$; Table 2). These correlations appeared to be driven primarily by AD men, in whom both NMDAR density and MMSE scores were reduced, confirmed when correlations were examined within sex and diagnostic groups: NMDAR levels in the CA1 were significantly and positively correlated with MMSE in AD men (CA1: $n = 20$, r = 0.67; Figure 3). Exploratory analyses in other regions revealed that NMDAR levels in the DG and the EC were also significantly and positively correlated with MMSE in AD men (DG: $n = 21$, r = 0.64, $p < 0.01$; EC: $n = 19$, r = 0.50, $p < 0.05$; Table 2). In contrast, there were no significant correlations between NMDAR density and MMSE in AD women or in men or women within the MCI and CN groups (Table 2). When we performed Fisher r-to-z comparisons of the independent Spearman coefficients [cocor, [34]], we found that the NMDAR-MMSE coupling in AD men differed significantly from that in AD women in the CA1 (z = 2.72, $p = 0.0066$) and DG (z = 2.91, $p = 0.0036$).

Table 2. Results from Spearman's correlations between NMDAR density and antemortem cognitive scores on the MMSE.

Regions	All Subjects r (*n*)	WOMEN				MEN			
		All r (*n*)	CN r (*n*)	MCI r (*n*)	AD r (*n*)	All r (*n*)	CN r (*n*)	MCI r (*n*)	AD r (*n*)
CA1	0.24 ** (124)	0.11 (59)	−0.04 (19)	−0.32 (21)	−0.15 (18)	0.36 ** (65)	0.17 (23)	0.19 (22)	0.67 **$ (20)
DG	0.02 (130)	−0.10 (62)	0.06 (20)	−0.17 (21)	−0.21 (21)	0.12 (68)	0.31 (23)	0 (24)	0.64 **$ (21)
S	0.06 (124)	−0.17 (60)	0.24 (19)	−0.10 (21)	−0.28 (19)	0.19 (64)	0.36 (23)	0.13 (22)	0.20 (19)
EC	0.10 (117)	0.04 (55)	−0.05 (18)	−0.01 (18)	0.04 (18)	0.16 (63)	0.13 (20)	0.08 (24)	0.50 * (19)
PC	0.11 (135)	0.15 (68)	−0.38(20)	−0.03(24)	0.35 (24)	0.09 (67)	0.07 (22)	0.24 (23)	−0.05 (22)

The correlation between NMDAR density in the CA1 and MMSE scores was hypothesis-driven and thus prespecified. All other regional correlations were considered exploratory. *r* = Spearman's correlation coefficient. * $p < 0.05$; ** $p < 0.01$. $ Correlation coefficient differs significantly between AD men and AD women (Fisher's r-to-z comparison of Spearman's correlation coefficients). CN, cognitively normal; MCI, mild cognitive impairment; AD, Alzheimer's disease; MMSE, Mini-

Mental State Examination; CA1, cornu ammonis field 1 of the hippocampus; DG, dentate gyrus; S, subiculum; EC, entorhinal cortex; PC, parietal cortex. *n* reflects the number of subjects with usable paired NMDAR–MMSE measurements for the indicated region.

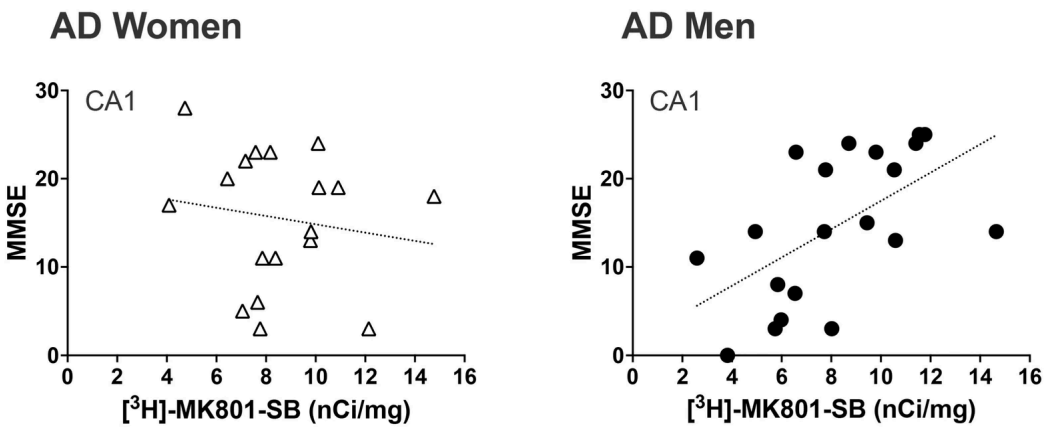


Figure 3. A significant positive correlation between MMSE scores and NMDA Receptor density in the CA1 of men but not women with Alzheimer's disease (AD). AD men, $n = 20$, $r = 0.67$, $p < 0.01$; AD women, $r = -0.15$, $n = 18$, $p > 0.05$. The NMDAR-MMSE coupling in AD men differed significantly from that in AD women (Fisher's r-to-z comparison of Spearman's correlation coefficients).

2.4. Tau Density Is Elevated in Alzheimer's Disease and Shows a Sex-Specific Regional Distribution

We sought to examine the relationship between NMDAR regional density and the core pathology of AD, namely the density of tau deposits. To this end, we performed quantitative in vitro autoradiography with [^{18}F]-T807 on consecutive sections from the same brain samples in which we measured NMDAR density. As expected, tau deposition was low to non-existent in the CN group, with low-to-moderate densities in the MCI group, and a high density in the entorhinal cortex in the AD group (Figure 4).

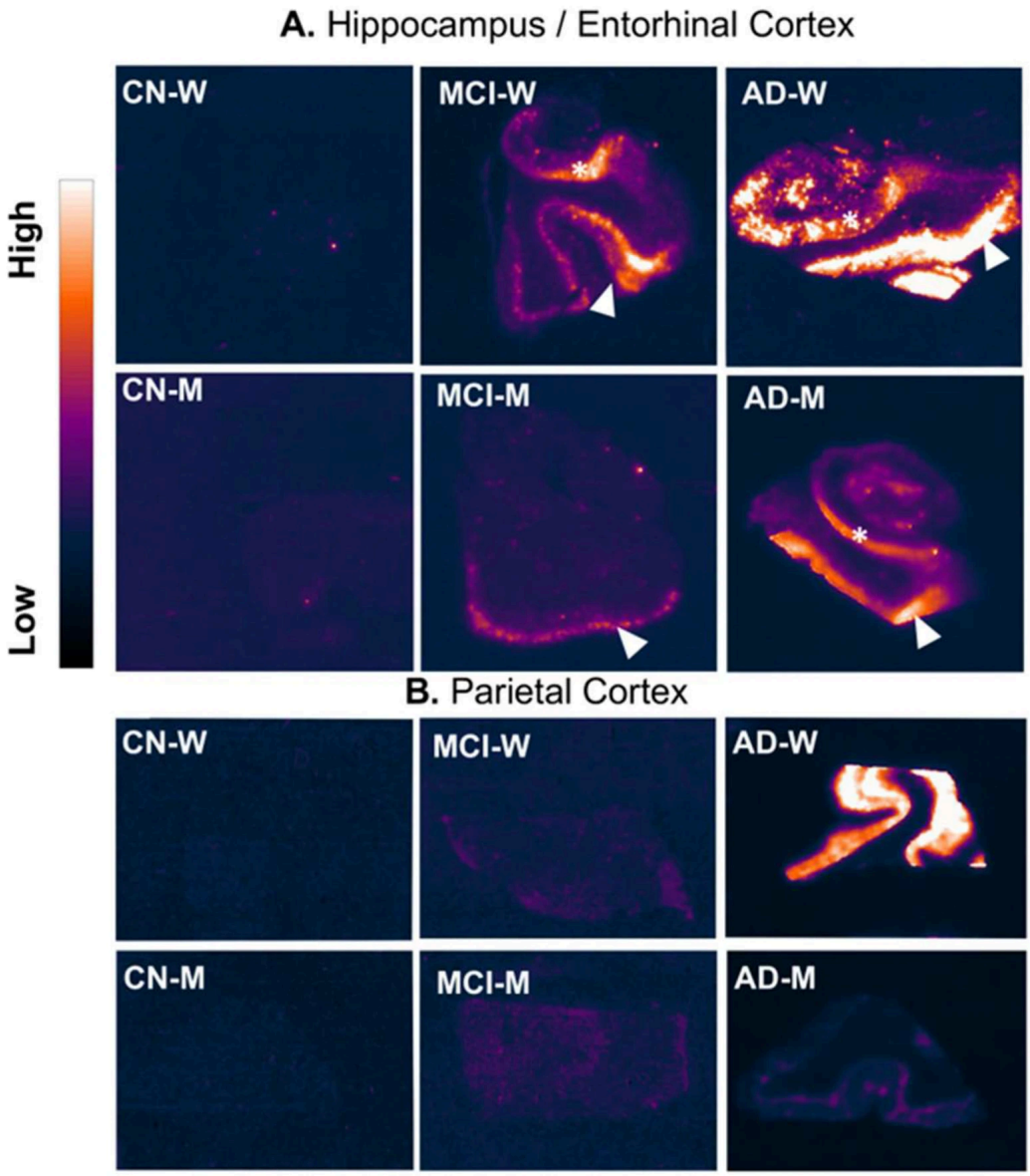


Figure 4. Densities of tau in the hippocampus, adjacent entorhinal cortex and the parietal cortex of CN, MCI, and AD women and men measured with [^{18}F]-T807 autoradiography. Panels depict representative pseudo-colored autoradiograms of tau labeled with [^{18}F]-T807 from the hippocampus and adjacent EC (panel (**A**)) and from the PC (panel (**B**)) of CN, MCI and AD subjects. Autoradiograms were pseudo-colored using the Gem lookup table (bar on the left). White arrows point to the EC and white asterisks point to the subiculum in MCI and AD subjects. Note the high tau density in the EC of both male and female AD subjects and in the PC of AD women. CN, cognitively normal; MCI, mild cognitive impairment; AD, Alzheimer's disease; EC, entorhinal cortex; PC, parietal cortex.

A three-way ANCOVA was conducted to analyze the effects of diagnosis, sex, and region on cube-root transformed tau density, while controlling for age and years of education (covariates). There was a significant effect of age ($p = 0.020$) and of years of education ($p = 0.005$) on tau density; both covariates were therefore retained in the final model. After covariate adjustment, there was a significant main effect of sex ($p < 0.001$), diagnosis ($p < 0.001$), and regions ($p < 0.001$) on tau density. There were also significant two- and three-way interactions of sex × diagnosis ($p < 0.001$), diagnosis × region ($p < 0.001$), and sex × diagnosis × region ($p = 0.034$). The sex x region interaction did not reach signifi-

cance (p = 0.110). Pairwise comparisons (Bonferroni-corrected) indicated that within the AD group, women showed a higher tau density than men (p < 0.001; Figures 4 4 and 5 5). Moreover, in women, tau density was significantly higher in the AD group relative to the CN and MCI groups (p < 0.001; Figure 5A), which did not differ from each other, while in men, tau density was significantly higher in the AD and the MCI groups relative to the CN group (men: AD > CN, p < 0.001; MCI > CN, p = 0.03; AD > MCI, p < 0.001). Subsequent analyses stratified by sex revealed significant main effects of diagnosis and region in both sexes, but only women showed a significant diagnosis x region interaction (p < 0.001). The diagnosis x region interaction in women was driven by higher cortical tau density relative to hippocampal subregions within the AD group (tau density in AD women: EC > CA1, p = 0.008; EC > DG, p < 0.001; PC > CA1, p < 0.001; PC > DG, p < 0.001; PC > S, p = 0.03; EC = PC). Figure 5 shows results stratified by sex with Bonferroni-corrected pairwise comparisons for each region.

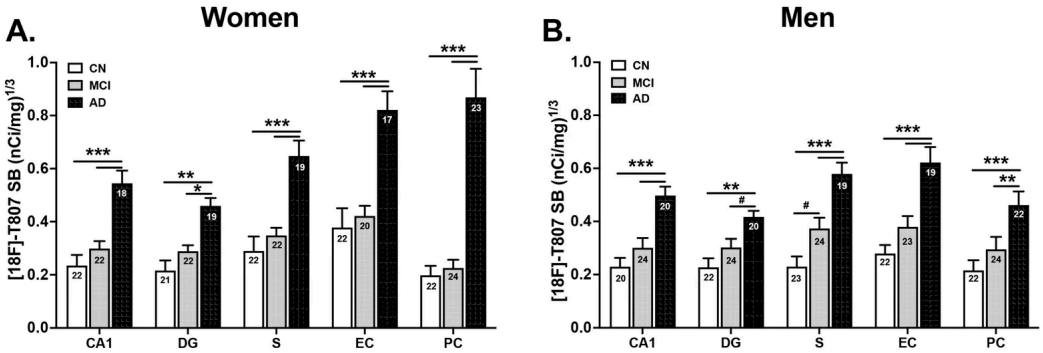


Figure 5. Tau densities are significantly elevated in hippocampal subregions and cortical regions of men and women with AD. Graphs depict quantitative autoradiographic measurements of tau density (expressed as specific binding of [^{18}F]-T807 in nCi/mg tissue) across diagnosis in women (**A**) and men (**B**). *** p < 0.001, ** p < 0.01, * p < 0.05, AD relative to controls or MCI, #, approaching significance, p = 0.06–0.07. Two-way ANCOVA with age and years of education as covariates followed by Bonferroni correction. Data are presented as mean ± SEM. Numbers inside bars denote the number of subjects with useful data per region and diagnosis. Abbreviations: CA1, cornu ammonis field 1 of the hippocampus; DG, dentate gyrus; S, subiculum; EC = entorhinal cortex; PC, parietal cortex; SB, specific binding; CN, cognitively normal; MCI, mild cognitive impairment; AD, Alzheimer's disease.

2.5. NMDA Receptor Density Is Negatively Correlated with Tau Density in Alzheimer's Disease Men

The vulnerability of the CA1 subfield to neurodegeneration in AD is thought to be mediated in part by its direct monosynaptic input from the EC and consequent EC-tau-related deafferentation [31–33,35–37]. Hence, pre-specified correlation analyses segregated by sex and by diagnostic group revealed a significant negative correlation in the EC of men with AD (n = 19, r = −0.60, p < 0.01), whereas in the CA1 negative correlations approached significance (n = 20, r = −0.44, p = 0.05; Table 3). In AD women, by contrast, the EC correlation between NMDAR and tau density was positive (n = 16, r = 0.46), and negative correlations in other regions approached significance only in the PC (n = 23, r = −0.38, p = 0.08). Fisher r-to-z transformation comparison confirmed that the EC correlation in AD men differed significantly from that in AD women, with the two coefficients running in opposite directions (z = −3.19, p = 0.0014).

Table 3. Spearman correlations between regional NMDAR and tau density, stratified by sex and diagnosis.

Regions	All Subjects r (*n*)	WOMEN				MEN			
		All r (*n*)	CN r (*n*)	MCI r (*n*)	AD r (*n*)	All r (*n*)	CN r (*n*)	MCI r (*n*)	AD r (*n*)
CA1	−0.12 (122)	−0.10 (69)	0.15 (21)	0 (22)	0.13 (17)	−0.14 (62)	0.17 (20)	0.19 (22)	−0.44 # (20)
DG	0 (127)	0 (62)	0.17 (21)	0.10 (22)	−0.21 (19)	0 (65)	−0.07 (21)	0.15 (24)	−0.34 # (20)
S	0 (124)	0.1 (61)	0 (21)	0.10 (22)	−0.18 (18)	−0.18 (63)	−0.05 (23)	−0.31 (22)	0 (18)
EC	−0.10 (115)	0 (54)	0.1 (20)	−0.21 (18)	0.46 # (16)	−0.11 (62)	0.1 (19)	0.26 (24)	−0.60 **$ (19)
PC	0 (137)	−0.14 (69)	0 (22)	0 (24)	−0.38 #(23)	0 (68)	0.16 (21)	0.1 (23)	0 (23)

Correlations between NMDAR and tau density in the CA1 and EC were hypothesis-driven and thus prespecified. All other regional correlations were considered exploratory. *r* = Spearman's correlation coefficient. ** $p < 0.01$; # $0.05 \leq p < 0.10$. $ Correlation coefficient differs significantly between AD men and AD women (Fisher's r-to-z comparison of Spearman's correlation coefficients). CN, cognitively normal; MCI, mild cognitive impairment; AD, Alzheimer's disease; CA1, cornu ammonis field 1 of the hippocampus; DG, dentate gyrus; S, subiculum; EC, entorhinal cortex; PC, parietal cortex. *n* reflects the number of subjects with usable paired NMDAR–tau measurements for the indicated region.

Interestingly, side-by-side comparisons of tau and NMDAR autoradiograms from consecutive sections of the same individuals revealed qualitatively distinct spatial patterns, with tau deposition appearing as puncta and clusters whereas NMDAR binding was comparatively continuous within regions. Representative images in Figure 6 suggest that areas with dense tau signals may correspond to areas of relatively lower NMDAR density, whereas areas with low or punctate tau signal may show relatively preserved NMDAR density. These distinct spatial patterns may have contributed to the limited number of statistically significant region-level correlations observed in our study.

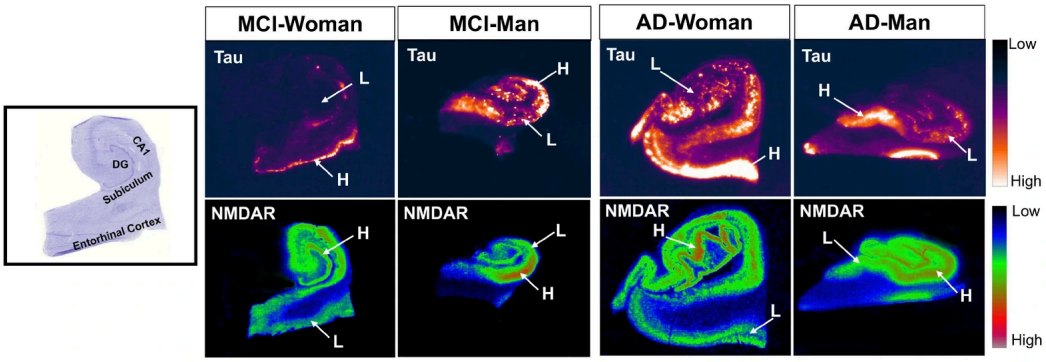


Figure 6. Representative spatial patterns of tau and NMDA receptor density in consecutive sections. Clusters of very high tau density coincide with locally lower NMDA receptor density within hippocampal and cortical regions. Top panels depict representative pseudo-colored autoradiograms of tau labeled with [^{18}F]-T807 from the hippocampus and adjacent entorhinal cortex of female and male MCI subjects and female and male AD subjects. Bottom panels show pseudo-colored autoradiograms of NMDA receptor labeled with [^{3}H]-MK801 from consecutive sections of the hippocampus and entorhinal cortex from the same subjects. Arrows indicate representative areas in which high (H) tau density appears to correspond to relatively lower (L) NMDAR density, whereas areas with low/punctate tau signal appear to show relatively higher NMDAR density. These comparisons are qualitative and were not assessed by pixel-level co-registration.

3. Discussion

In this quantitative autoradiographic study of NMDAR in hippocampal and cortical regions across the AD continuum, we show that a clinical diagnosis of AD is associated

with lower NMDA receptor density in the hippocampus of both women and men, with the most pronounced loss in the CA1 field. Among subjects with a diagnosis of MCI, women, but not men, exhibit lower NMDAR density relative to age-matched controls. Lower NMDAR densities are associated with poor antemortem cognitive performance as measured by the MMSE. Moreover, higher tau density is associated with lower NMDAR density, with significant associations localized to the EC of AD men.

The fate of NMDAR in the brain of subjects with AD has been the subject of a number of previous studies. Using L-[^{3}H]-glutamate binding to sections from the hippocampal formation of six patients who died from dementia of the Alzheimer's type (DAT) and six patients without DAT, Greenamyre et al. [20] found marked reductions in total [^{3}H]-glutamate binding in all regions of hippocampus and adjacent parahippocampal cortex in DAT brains as compared to controls. When subtypes of excitatory amino acid receptors were assayed, it was found that binding to the N-methyl-D-aspartate (NMDA)-sensitive receptor was most markedly reduced, with the greatest loss found in the stratum moleculare and stratum pyramidale of CA1. We replicated and extended these findings in a subsequent autoradiographic study showing reduced NMDAR binding in the CA1 of subjects who died with AD which tracked disease severity by Braak stage and was negatively correlated with neuroinflammation [23]. In a recent study, lower levels of synaptic NMDAR subtypes GluN2B and GluN2A were found in AD synaptic membrane fractions, whereas extrasynaptic GluN2B and GluN1 levels were significantly higher in AD [25]. This apparent contradiction may suggest that both decreases and increases in NMDAR density may occur, either sequentially or in parallel, in different subcellular locations and stages of disease progression and may also be modulated by sex [38].

To elaborate, there is a near-consensus that synaptic loss is an early event in AD [39–42]. Synaptic degeneration and the ensuing loss of contacts results in sustained decreases in NMDAR stimulation, impairing synaptic plasticity in the form of LTP and long-term depression (LTD), both necessary for learning and memory [2,6,14]. Conversely, sustained reductions in synaptic transmission—through persistent decreases in NMDAR stimulation—can also drive compensatory upregulation of NMDARs. This has been demonstrated by in vitro and in vivo radioligand-binding studies in which a reduction in NMDAR stimulation in the form of chronic antagonist treatment leads to an upregulation of NMDAR densities [33–36]. In fact, postmortem studies have shown upregulation of NMDAR subunits (i.e., GluN1, GluN2B) in the early stages (Braak II) of AD [16]. Other studies suggest that increased NMDAR density early in AD may reflect upregulation of extrasynaptic receptors, whose low but continuous stimulation contributes to synaptic impairment [43]. Hence, the changes in NMDAR densities reported in our study likely reflect both a compensatory mechanism observed in the early stages of AD, as well as an altered function of synaptic/extrasynaptic NMDARs that initiate hyperactivation and eventual excitotoxicity, with the end result being the loss of NMDAR positive neurons tipping the balance towards lower receptor density in advanced AD.

With regard to sex differences in NMDAR density, we uncovered a sex-divergent pattern in the loss of NMDAR among women and men with MCI: in the CA1, MCI women showed an NMDAR density comparable to AD levels and lower than age-matched CN, whereas MCI men showed NMDAR levels slightly higher than age-matched CN and significantly higher than AD men. Mild cognitive impairment is considered a transitional stage from healthy aging to dementia, in which individuals—while still capable of performing activities of daily living—experience subtle but measurable cognitive deficits [44]. The fact that MCI women and not MCI men are already showing a loss of NMDARs is consistent with studies demonstrating that compared to men, women experienced a greater pathological burden at earlier stages of the disease [45–49].

In fact, women decline faster from MCI to AD [50,51] and demonstrate heightened sensitivity to tau deposition [52,53] and neuroinflammation [54,55]. In a recent longitudinal study by our group, we show that in the MCI stage, women exhibit a significantly steeper memory decline associated with increasing cerebrospinal fluid (CSF) phosphorylated tau 181 (pTau181/amyloid b42 (Ab42) ratios compared to men [27]. Therefore, the decrease in NMDAR density observed in MCI women might be another biological mechanism contributing to their steeper cognitive decline relative to men.

Surprisingly, while initial analyses that included all subjects revealed significant positive correlations between antemortem MMSE scores and CA1 NMDAR density, subsequent analyses stratified by sex and diagnosis showed that AD men—particularly the lower cognitive performers—drove this positive relationship. Although this pattern initially appears counter-intuitive given that women bear a disproportionately greater AD burden, it is consistent with the growing literature documenting sex-specific coupling between pathology and cognition. Women appear to tolerate more tau pathology before verbal-memory decline emerges [56], and in a multicenter memory clinic cohort spanning the full clinical spectrum, the association between tau load and cognitive performance was significantly stronger in men than in women, despite women showing a greater tau burden overall [57]. By analogy, our NMDAR–MMSE finding suggests that in men—who may lack the compensatory or reserve mechanisms invoked by women—molecular measures of synaptic integrity map more directly onto cognitive performance. Whether this reflects diminished reserve or differential downstream sensitivity to receptor loss remains an important question for future study. Notably, the persistence of this male-specific coupling into the AD-dementia stage—rather than being confined to earlier, preclinical stages—suggests that sex differences in pathology–cognition coupling may not be strictly stage-limited, and longitudinal designs tracking both sexes across the full AD continuum will be needed to disentangle stage-specific from sex-specific contributions to this pattern.

Consistent with our a priori hypothesis, in both sexes, the AD-related decrease in NMDAR density was most pronounced in CA1. The CA1 vulnerability is in line with a substantial body of evidence from in vivo imaging and postmortem histological studies of AD, which consistently show selective vulnerability of the CA1 to volume loss and neuronal death relative to other hippocampal subfields [28–30,58,59]. In addition, ample literature demonstrates selective vulnerability of the CA1 in response to insults including excitotoxicity and ischemia [30,60], and offers multiple explanations for this phenomenon [61,62]. Moreover, in women and men with AD, we observed high tau deposition in the EC, which is the first cortical region to show significant tau deposition (Braak stages I–II; [35]). The CA1 region has direct, monosynaptic excitatory input from the EC [32,33,36,37]. This direct input is thought to create a neuronal pathway for the propagation of tau pathology from EC to CA1, with tau toxicity driving early neuronal death and neurodegeneration [31]. Because the EC serves as the major gateway for cortical input into the hippocampus, tau-induced damage to EC projection neurons deprives CA1 of its principal excitatory drive, contributing to CA1 functional isolation, neurodegeneration, and cell death.

In agreement with previous findings, we showed AD-related increases in tau density in all regions examined, with AD women demonstrating higher tau density relative to AD men [52–54]. Moreover, in women, there was a significant region-by-diagnosis interaction caused by prominent increases in the EC, the site of initial cortical tau deposition in AD, and in the PC, a region that shows tau deposition only at more advanced stages of the disease. In vitro and in vivo studies have shown complex interactions between tau and NMDARs, with studies suggesting that under pathological states, tau ac-

cumulation impairs synaptic plasticity through JAK2/STAT1-induced suppression of NMDAR expression [14]. However, despite the highly significant tau deposition in our AD subjects, tau density was significantly associated with decreased NMDAR density only in the EC of AD men, whereas in AD women, a negative association between tau and NMDAR density approached significance only in the PC. Taken together with the male-specific correlation between CA1 NMDAR density and MMSE scores in AD, this pattern suggests that in men, NMDAR loss may be more directly linked to tau-related neurodegeneration and consequent cognitive impairment, whereas in women these relationships may be more multifactorial or partly uncoupled from NMDAR density, potentially reflecting a broader set of pathological processes contributing to cognitive decline. One candidate contributor is neuroinflammation, which we have previously shown tracks NMDAR loss in the hippocampus [23] and shows sex- and region-dependent patterns in AD [54]; given the established bidirectional relationship between tau pathology and neuroinflammation, this may help explain the less direct tau–NMDAR coupling observed in women. We speculate that the lack of significant negative associations between tau and NMDAR density in additional regions is due to qualitative differences in the density patterns of these two markers within regions, whereby punctate tau deposition is often associated with preserved NMDAR density, while dense and confluent tau accumulation coincides with locally reduced NMDAR density. Nevertheless, the fact that negative correlations were found in regions with the highest tau density in women (PC) and in men (EC) is consistent with previous reports in which hippocampal protein levels and mRNA expression for specific NMDAR subunits, such as GluN1/GluN2B, are reduced with increasing AD-related neuropathology (Braak stage; [3]).

Several limitations should be considered when interpreting these findings. First, the cross-sectional postmortem design permits comparisons among CN, MCI, and AD groups but cannot establish within-subject trajectories of receptor change during disease progression. In addition, the MCI groups were older on average than the CN and AD groups in both sexes, an atypical age distribution that may reflect characteristics of postmortem cohort recruitment and survival. Although age was not a significant covariate of NMDAR density, this sampling characteristic should be considered when interpreting diagnostic-group comparisons. Finally, although the AD-related reduction in NMDAR density was most pronounced in the CA1, the absence of a significant diagnosis x region interaction precludes definitive conclusions regarding regional specificity. Longitudinal studies will be required to determine whether the sex-specific patterns observed here reflect differential trajectories of NMDAR during AD progression.

4. Materials and Methods

4.1. Sample Characteristics and Handling

The current study used 10-micron-thick sections of fresh-frozen samples of the hippocampus/entorhinal cortex and the parietal cortex from 154 donors equally divided among men and women and the three diagnostic groups (Control, MCI and AD). One hundred and seventeen samples (18–20 per sex/diagnosis) were obtained from the Arizona Study of Aging and Neurodegenerative Disorders and Brain and Body Donation Program (BBDP) [63] and 37 samples (6–7 per sex/diagnosis) from the University of Washington BioRepository and Integrated Neuropathology (BRaIN) repository. Cases that were given a neuropathological diagnosis of a neurodegenerative disease other than AD were excluded. Inclusion criteria were complete neuropathological examination (e.g., Braak staging, Thal amyloid staging) and a comprehensive antemortem neurocognitive evaluation that indicated a clinical diagnosis of either cognitively normal, MCI or AD dementia as recently described [54]. For BRaIN subjects, cog-

nitive evaluations were required to be within 18 months of death; for BBDP subjects, diagnoses were based on the closest available evaluation from the National Alzheimer's Coordinating Center (NACC) Uniform Data Set battery. Pathological data confirmed the presence of AD dementia or its absence for control and MCI groups, although control or MCI subjects could have some degree of incidental pathology. For most subjects, ApoE genotype was also provided (Table 1). Post mortem interval (PMI) was less than 12 h for all samples (Table 1). Upon reception, samples were stored in a −80 °C freezer until use. All frozen samples were cryo-sectioned (Leica cm 1950) at −20 °C (10 μm) in 10 consecutive series and thaw-mounted onto positively charged glass slides (Fisher Scientific, MA, USA).

Tissue was received in separate shipments comprising 36 subjects balanced by sex and diagnosis (6 subjects/sex/diagnostic group). For each radioligand, one hippocampus/entorhinal cortex section per subject was included in a 36-slide labeling experiment, and a separate 36-slide experiment was performed using parietal cortex sections from the same subjects; additional slides were included for determination of nonspecific binding. Within each experiment, slides were randomly allocated across autoradiographic films (typically three films per experiment), such that film allocation was independent of sex and diagnosis.

4.2. In Vitro Quantitative Autoradiography

The labeling of NMDAR on tissue sections was done as described previously [23]. Briefly, on the day of the assay, consecutive slides from each subject were removed from the −80 °C freezer and allowed to reach room temperature. After a 30 min prewash in 50 mM Tris-acetate buffer (pH 7.4), the sections were incubated for 3 h at room temperature in 50 mM Tris-acetate buffer at pH 7.4 containing 5 nM [^{3}H]MK801 (a selective non-competitive NMDAR antagonist; specific activity 27.5 Ci/mmol, PerkinElmer Life Sciences, Waltham, MA, USA), 30 μM glutamate, and 10 μM glycine. The inclusion of saturating concentrations of glutamate (30 μM) and glycine (10 μM) in the assay ensures that all NMDARs are in the activated, channel-open conformation required for MK801 binding; under these conditions, the density of MK801-labeled sites is equivalent to the total receptor density, rather than reflecting the proportion of receptors in an activated state [64]. Nonspecific binding was determined in the presence of 10 μM unlabeled MK801. At the end of the incubation, the sections were dipped for 5 s in ice-cold buffer and then washed for 90 min in cold, fresh buffer, followed by a dip in ice-cold double-distilled water. Sections were then dried on a slide warmer at 60 °C and apposed to low-energy radiation sensitive film (BluBlot^{TM} HS, Chemglass, NJ, USA), for 8 weeks, alongside calibrated tritium microscales (Amersham Pharmacia Biotech, Inc., Piscataway, NJ, USA). Films were developed in Kodak D-19, fixed, and dried. To assess tau deposits autoradiography was performed with [^{18}F]-T807 obtained from the Stony Brook University PET radiochemistry laboratory. Sections were transferred to a bath containing ~2 nM [^{18}F]-T807 in 10 mM phosphate-buffered saline (PBS). After incubation for 60 min, slides were washed in 10 mM PBS for 1 min, 70% ethanol/30% PBS for 2 min, 30% ethanol/70% PBS for 1 min, and lastly in PBS for 1 min [54]. Slides were then air dried, apposed to film for 1 h and developed as described above. The regions examined in this study (hippocampus, entorhinal cortex, and parietal cortex) do not include the principal sites of off-target [^{18}F]-T807 binding—namely the basal ganglia (MAO-B-rich) and substantia nigra (neuromelanin-rich). The regional and subcellular specificity of [^{18}F]-T807 for paired helical filament tau has been extensively validated against AT8 immunohistochemistry in postmortem hippocampus, cortex, and amygdala using both macroscopic (phosphor-screen) and microscopic (nuclear emulsion) autoradiography, with excellent concordance be-

tween tracer signal and neurofibrillary tangle distribution [65]. All sections were cresyl violet-stained for histology after film development.

4.3. Quantitative Image Analysis

Developed films were scanned using a flatbed scanner (2400 dpi, 256 gray levels, in neutral conditions—no highlights, shadows, midtones, gamma or sharpen manipulations), digitized and saved in 8-bit Tiff format. Quantitative image analyses were performed using the FIJI (NIH Image) software. Regions of interest (ROIs) in hippocampus samples were identified in reference to the histological staining and an atlas of the human hippocampus [66] and included the cornu ammonis field 1 (CA1), dentate gyrus (DG), subiculum (S), entorhinal cortex (EC) and parietal cortex (PC). ROIs were manually drawn on the autoradiograms around the whole extent of each region on all sections where the region could be clearly distinguished on the histologically stained section. Nonspecific binding was subtracted from total binding to generate specific binding values for statistical analysis.

Image analysis of autoradiograms and statistical analysis of the results from each experiment were performed by an investigator blinded to sex and diagnosis and then decoded by the senior investigators (MAM and AB).

4.4. Statistical Analysis

Prior to modeling, distributional assumptions were examined using skewness and kurtosis values as well as the Shapiro–Wilk test. Tau density values were cube-root transformed to meet assumptions of normality. Homogeneity of variance was tested for all continuous variables using Levene's test. Demographic data were analyzed using a two-way ANOVA with sex and diagnosis as factors. ApoE genotype was dichotomized into Apoε4 carriers and non-carriers, and Fisher's exact tests were used to examine diagnosis effects.

For each autoradiographic marker (NMDAR density, tau density), the effects of diagnosis, sex and region were evaluated by a three-way ANCOVA with age and years of education as candidate covariates. Covariates were initially evaluated in a full model and retained in the final model only when they exerted a significant effect ($p < 0.05$) on the dependent variable; when neither covariate reached significance, a three-way ANOVA without covariates was used. Under this rule, age and years of education were retained for tau density but not for NMDAR density. When a significant sex × diagnosis or sex × diagnosis × region interaction was detected, sex-stratified two-way ANOVA (or ANCOVA as appropriate) was performed with diagnosis and region as fixed factors. Pairwise post-hoc comparisons were corrected with the Bonferroni method.

Because tissue samples were obtained from two repositories, repository (BBPD vs. BRAIN) was additionally evaluated as a potential source effect. Repository did not significantly affect NMDAR density and did not alter the principal effects of diagnosis or sex × diagnosis interaction (ANOVA, $p > 0.05$, as covariate or as main fixed factor).

As a sensitivity analysis to account for within-donor dependence among regional NMDAR measurements, we additionally fitted a linear mixed model with region modeled as a repeated factor within donor using a compound-symmetry covariance structure and Satterthwaite degrees of freedom. Sex, diagnosis, region, and their interactions were included as fixed effects. Follow-up simple-effects analyses examined diagnosis effects within each sex and region, with Bonferroni adjustment for pairwise comparison.

Given the modest within-group sample sizes (n = 18–23 per sex × diagnosis cell) and the restricted, ceiling-affected distribution of MMSE scores, associations between regional NMDAR density and MMSE, and between regional NMDAR and tau density,

were assessed with Spearman's rank correlation. Correlation sample sizes were lower than full diagnostic-group sizes (Table 1) because cryosectioning, labeling, and technical exclusion occasionally resulted in the loss of specific regional measurements in individual subjects. Because correlation analyses required usable paired measurements, the loss of a regional measurement for either variable reduced the sample size available for the corresponding correlation.

Image analyses of autoradiograms and preliminary statistical analyses were performed by an investigator blinded to sex and diagnosis; group codes were revealed only for final interpretation by the senior investigators (MAM and AB).

All statistical analyses were performed using SPSS Statistics version 28 (IBM Corp., Armonk, NY, USA); graphs were prepared with GraphPad Prism 9 (GraphPad Software, San Diego, CA, USA). Statistical significance was set at $\alpha = 0.05$. Data are presented as mean ± SEM unless otherwise noted.

5. Conclusions

NMDA receptor density is strongly modulated by sex, region and AD disease stage. Antemortem cognitive scores in men were more sensitive to the loss of NMDAR. These findings may contribute to the understanding of the known sex differences in AD prevalence, presentation and progression.

Author Contributions: Conceptualization, M.A.-M., A.B., and E.E.S.; methodology, S.M. and J.D.; validation, M.A.-M., A.B., and S.M.; investigation, S.M., V.C., A.N., and J.D..; resources, G.E.S., T.G.B. and M.A.-M.; data curation, M.A.-M.; writing, M.A.-M. and A.B.; review and editing, E.E.S.; visualization, M.A.-M.; supervision, M.A.-M. and A.B.; project administration, M.A.-M.; funding acquisition, E.E.S. All authors have read and agreed to the published version of the manuscript.

Funding: This study was supported by R01 AG074221-01 (E.E. Sundermann, PI). Anat Biegon was supported in part by a fellowship from the Swedish collegium for Advanced Studies (SCAS). The Brain and Body Donation Program has been supported by the National Institute of Neurological Disorders and Stroke (U24 NS072026 National Brain and Tissue Resource for Parkinson's Disease and Related Disorders), the National Institute on Aging (P30 AG019610 and P30AG072980, Arizona Alzheimer's Disease Center), the Arizona Department of Health Services (contract 211002, Arizona Alzheimer's Research Center), the Arizona Biomedical Research Commission (contracts 4001, 0011, 05-901 and 1001 to the Arizona Parkinson's Disease Consortium), and the Michael J. Fox Foundation for Parkinson's Research.

Institutional Review Board Statement: This work was done at Stony Brook University using de-identified human tissue samples collected under approved protocols by established tissue repositories, namely the University of Washington (UW) BioRepository and Integrated Neuropathology laboratory (BraIN; https://dlmp.uw.edu/research-labs/keene/BRaIN-lab access on 30 June 2026) and the Arizona Study of Aging and Neurodegenerative Disorders and Brain and Body Donation Program (BBDP; www.brainandbodydonation program.org) after approval by their respective institutional review boards. The Stony Brook University investigators received only de-identified tissue and associated data, without direct identifiers or coded links permitting identification of individual donors. Accordingly, under the U.S. Department of Health and Human Services definition of a human subject (45 CFR §46.102(e)), the secondary analyses conducted at Stony Brook University did not constitute human-subjects research and did not require additional IRB review or informed consent.

Informed Consent Statement: Human brain tissue was obtained from the University of Washington BioRepository and Integrated Neuropathology (BraIN) Laboratory and the Arizona Study of Aging and Neurodegenerative Disorders and Brain and Body Donation Program (Banner

Sun Health Research Institute). All tissue collection and autopsy procedures were conducted under protocols approved by the local Institutional Review Boards at the University of Washington and Banner Health, with informed consent obtained from participants or their next of kin, in accordance with the Declaration of Helsinki.

Data Availability Statement: The raw data supporting the conclusions of this article will be made available by the authors on request.

Conflicts of Interest: The authors declare no conflicts of interest.

Abbreviations

The following abbreviations are used in this manuscript: CN, cognitively normal; MCI, mild cognitive impairment; AD, Alzheimer's disease; NMDAR, N-methyl-D-aspartate receptor; EC, entorhinal cortex; PC, parietal cortex; S, subiculum; CA1, cornu ammonis field 1; DG, dentate gyrus; MMSE, Mini-mental State Examination test; LTP, long-Term Potentiation; LTD, long-term depression; PMI, postmortem Interval; CSF, cerebrospinal fluid; ROI, Region of interest; PBS, phosphate-buffered saline

References

1. Castellano, C.; Cestari, V.; Ciamei, A. NMDA receptors and learning and memory processes. *Curr. Drug Targets* **2001**, *2*, 273–283. [Google Scholar] [CrossRef]
2. Newcomer, J.W.; Krystal, J.H. NMDA receptor regulation of memory and behavior in humans. *Hippocampus* **2001**, *11*, 529–542. [Google Scholar] [CrossRef]
3. Mishizen-Eberz, A.J.; Rissman, R.A.; Carter, T.L.; Ikonomovic, M.D.; Wolfe, B.B.; Armstrong, D.M. Biochemical and molecular studies of NMDA receptor subunits NR1/2A/2B in hippocampal subregions throughout progression of Alzheimer's disease pathology. *Neurobiol. Dis.* **2004**, *15*, 80–92. [Google Scholar] [CrossRef]
4. Aronica, E.; Dickson, D.W.; Kress, Y.; Morrison, J.H.; Zukin, R.S. Non-plaque dystrophic dendrites in Alzheimer hippocampus: A new pathological structure revealed by glutamate receptor immunocytochemistry. *Neuroscience* **1998**, *82*, 979–991. [Google Scholar] [CrossRef]
5. Babaei, P. NMDA and AMPA receptors dysregulation in Alzheimer's disease. *Eur. J. Pharmacol.* **2021**, *908*, 174310. [Google Scholar] [CrossRef]
6. Dong, B.; Yue, Y.; Dong, H.; Wang, Y. N-methyl-D-aspartate receptor hypofunction as a potential contributor to the progression and manifestation of many neurological disorders. *Front. Mol. Neurosci.* **2023**, *16*, 1174738. [Google Scholar] [CrossRef]
7. Soares, C.; Da Ros, L.U.; Machado, L.S.; Rocha, A.; Lazzarotto, G.; Carello-Collar, G.; De Bastiani, M.A.; Ferrari-Souza, J.P.; Lussier, F.Z.; Souza, D.O.; et al. The glutamatergic system in Alzheimer's disease: A systematic review with meta-analysis. *Mol. Psychiatry* **2024**, *29*, 2261–2273. [Google Scholar] [CrossRef]
8. Alfaro-Ruiz, R.; Aguado, C.; Martin-Belmonte, A.; Moreno-Martinez, A.E.; Merchan-Rubira, J.; Hernandez, F.; Avila, J.; Fukazawa, Y.; Lujan, R. Different modes of synaptic and extrasynaptic NMDA receptor alteration in the hippocampus of P301S tau transgenic mice. *Brain Pathol.* **2023**, *33*, e13115. [Google Scholar] [CrossRef]
9. Amadoro, G.; Ciotti, M.T.; Costanzi, M.; Cestari, V.; Calissano, P.; Canu, N. NMDA receptor mediates tau-induced neurotoxicity by calpain and ERK/MAPK activation. *Proc. Natl. Acad. Sci. USA* **2006**, *103*, 2892–2897. [Google Scholar] [CrossRef]
10. Goto, Y.; Niidome, T.; Akaike, A.; Kihara, T.; Sugimoto, H. Amyloid beta-peptide preconditioning reduces glutamate-induced neurotoxicity by promoting endocytosis of NMDA receptor. *Biochem. Biophys. Res. Commun.* **2006**, *351*, 259–265. [Google Scholar] [CrossRef]
11. Italia, M.; Ferrari, E.; Diluca, M.; Gardoni, F. NMDA and AMPA Receptors at Synapses: Novel Targets for Tau and alpha-Synuclein Proteinopathies. *Biomedicines* **2022**, *10*, 1550. [Google Scholar] [CrossRef]
12. Kobayashi, S.; Tanaka, T.; Soeda, Y.; Almeida, O.F.X.; Takashima, A. Local Somatodendritic Translation and Hyperphosphorylation of Tau Protein Triggered by AMPA and NMDA Receptor Stimulation. *EBioMedicine* **2017**, *20*, 120–126. [Google Scholar] [CrossRef]
13. Lesne, S.; Ali, C.; Gabriel, C.; Croci, N.; MacKenzie, E.T.; Glabe, C.G.; Plotkine, M.; Marchand-Verrecchia, C.; Vivien, D.; Buisson, A. NMDA receptor activation inhibits alpha-secretase and promotes neuronal amyloid-beta production. *J. Neurosci.*

2005, *25*, 9367–9377. [Google Scholar] [CrossRef]
14. Li, X.G.; Hong, X.Y.; Wang, Y.L.; Zhang, S.J.; Zhang, J.F.; Li, X.C.; Liu, Y.C.; Sun, D.S.; Feng, Q.; Ye, J.W.; et al. Tau accumulation triggers STAT1-dependent memory deficits by suppressing NMDA receptor expression. *EMBO Rep.* **2019**, *20*, EMBR201847202. [Google Scholar] [CrossRef]
15. Mondragon-Rodriguez, S.; Trillaud-Doppia, E.; Dudilot, A.; Bourgeois, C.; Lauzon, M.; Leclerc, N.; Boehm, J. Interaction of endogenous tau protein with synaptic proteins is regulated by N-methyl-D-aspartate receptor-dependent tau phosphorylation. *J. Biol. Chem.* **2012**, *287*, 32040–32053. [Google Scholar] [CrossRef]
16. Ortiz-Sanz, C.; Balantzategi, U.; Quintela-Lopez, T.; Ruiz, A.; Luchena, C.; Zuazo-Ibarra, J.; Capetillo-Zarate, E.; Matute, C.; Zugaza, J.L.; Alberdi, E. Amyloid beta / PKC-dependent alterations in NMDA receptor composition are detected in early stages of Alzheimer s disease. *Cell Death Dis.* **2022**, *13*, 253. [Google Scholar] [CrossRef]
17. Pallas-Bazarra, N.; Draffin, J.; Cuadros, R.; Antonio Esteban, J.; Avila, J. Tau is required for the function of extrasynaptic NMDA receptors. *Sci. Rep.* **2019**, *9*, 9116. [Google Scholar] [CrossRef]
18. Snyder, E.M.; Nong, Y.; Almeida, C.G.; Paul, S.; Moran, T.; Choi, E.Y.; Nairn, A.C.; Salter, M.W.; Lombroso, P.J.; Gouras, G.K.; et al. Regulation of NMDA receptor trafficking by amyloid-beta. *Nat. Neurosci.* **2005**, *8*, 1051–1058. [Google Scholar] [CrossRef]
19. Sun, X.Y.; Tuo, Q.Z.; Liuyang, Z.Y.; Xie, A.J.; Feng, X.L.; Yan, X.; Qiu, M.; Li, S.; Wang, X.L.; Cao, F.Y.; et al. Extrasynaptic NMDA receptor-induced tau overexpression mediates neuronal death through suppressing survival signaling ERK phosphorylation. *Cell Death Dis.* **2016**, *7*, e2449. [Google Scholar] [CrossRef]
20. Greenamyre, J.T.; Penney, J.B.; D'Amato, C.J.; Young, A.B. Dementia of the Alzheimer's type: Changes in hippocampal L-[3H]glutamate binding. *J. Neurochem.* **1987**, *48*, 543–551. [Google Scholar] [CrossRef]
21. Jansen, K.L.; Faull, R.L.; Dragunow, M.; Synek, B.L. Alzheimer's disease: Changes in hippocampal N-methyl-D-aspartate, quisqualate, neurotensin, adenosine, benzodiazepine, serotonin and opioid receptors--an autoradiographic study. *Neuroscience* **1990**, *39*, 613–627. [Google Scholar] [CrossRef]
22. Ulas, J.; Brunner, L.C.; Geddes, J.W.; Choe, W.; Cotman, C.W. N-methyl-D-aspartate receptor complex in the hippocampus of elderly, normal individuals and those with Alzheimer's disease. *Neuroscience* **1992**, *49*, 45–61. [Google Scholar] [CrossRef]
23. Kravitz, E.; Gaisler-Salomon, I.; Biegon, A. Hippocampal glutamate NMDA receptor loss tracks progression in Alzheimer's disease: Quantitative autoradiography in postmortem human brain. *PLoS ONE* **2013**, *8*, e81244. [Google Scholar] [CrossRef]
24. Brown, D.R.; Wyper, D.J.; Owens, J.; Patterson, J.; Kelly, R.C.; Hunter, R.; McCulloch, J. 123Iodo-MK-801: A spect agent for imaging the pattern and extent of glutamate (NMDA) receptor activation in Alzheimer's disease. *J. Psychiatr. Res.* **1997**, *31*, 605–619. [Google Scholar] [CrossRef]
25. Escamilla, S.; Badillos, R.; Comella, J.X.; Sole, M.; Perez-Otano, I.; Mut, J.V.S.; Saez-Valero, J.; Cuchillo-Ibanez, I. Synaptic and extrasynaptic distribution of NMDA receptors in the cortex of Alzheimer's disease patients. *Alzheimers Dement.* **2024**, *20*, 8231–8245. [Google Scholar] [CrossRef]
26. Emrani, S.; Sundermann, E.E. Sex/gender differences in the clinical trajectory of Alzheimer's disease: Insights into diagnosis and cognitive reserve. *Front. Neuroendocrinol.* **2025**, *77*, 101184. [Google Scholar] [CrossRef]
27. Sundermann, E.E.; Banks, S.J.; Bondi, M.W.; Martinez, M.A.; Biegon, A.; Rotblatt, L.J.; Hildebrandt, T. Sex differences in the relationship of biomarker change to memory decline in early Alzheimer's disease: An observational cohort study. *Biol. Sex. Differ.* **2026**, *17*, 38. [Google Scholar] [CrossRef]
28. Bartsch, T.; Dohring, J.; Reuter, S.; Finke, C.; Rohr, A.; Brauer, H.; Deuschl, G.; Jansen, O. Selective neuronal vulnerability of human hippocampal CA1 neurons: Lesion evolution, temporal course, and pattern of hippocampal damage in diffusion-weighted MR imaging. *J. Cereb. Blood Flow. Metab.* **2015**, *35*, 1836–1845. [Google Scholar] [CrossRef]
29. Bobinski, M.; de Leon, M.J.; Tarnawski, M.; Wegiel, J.; Reisberg, B.; Miller, D.C.; Wisniewski, H.M. Neuronal and volume loss in CA1 of the hippocampal formation uniquely predicts duration and severity of Alzheimer disease. *Brain Res.* **1998**, *805*, 267–269. [Google Scholar] [CrossRef]
30. Butler, T.R.; Self, R.L.; Smith, K.J.; Sharrett-Field, L.J.; Berry, J.N.; Littleton, J.M.; Pauly, J.R.; Mulholland, P.J.; Prendergast, M.A. Selective vulnerability of hippocampal cornu ammonis 1 pyramidal cells to excitotoxic insult is associated with the expression of polyamine-sensitive N-methyl-D-asparate-type glutamate receptors. *Neuroscience* **2010**, *165*, 525–534. [Google Scholar] [CrossRef]
31. Delpech, J.C.; Pathak, D.; Varghese, M.; Kalavai, S.V.; Hays, E.C.; Hof, P.R.; Johnson, W.E.; Ikezu, S.; Medalla, M.; Luebke, J.I.; et al. Wolframin-1-expressing neurons in the entorhinal cortex propagate tau to CA1 neurons and impair hippocampal memory in mice. *Sci. Transl. Med.* **2021**, *13*, eabe8455. [Google Scholar] [CrossRef]

32. Hernandez-Frausto, M.; Vivar, C. Entorhinal cortex-hippocampal circuit connectivity in health and disease. *Front. Hum. Neurosci.* **2024**, *18*, 1448791. [Google Scholar] [CrossRef]
33. Karimani, F.; Asgari Taei, A.; Abolghasemi-Dehaghani, M.R.; Safari, M.S.; Dargahi, L. Impairment of entorhinal cortex network activity in Alzheimer's disease. *Front. Aging Neurosci.* **2024**, *16*, 1402573. [Google Scholar] [CrossRef]
34. Diedenhofen, B.; Musch, J. cocor: A comprehensive solution for the statistical comparison of correlations. *PLoS ONE* **2015**, *10*, e0121945, Erruatm in *PLoS ONE* **2015**, *10*, e0131499. https://doi.org/10.1371/journal.pone.0131499. [Google Scholar] [CrossRef]
35. Braak, H.; Braak, E. Neuropathological stageing of Alzheimer-related changes. *Acta Neuropathol.* **1991**, *82*, 239–259. [Google Scholar] [CrossRef]
36. Shu, S.; Zhu, H.; Tang, N.; Chen, W.; Li, X.; Li, H.; Pei, L.; Liu, D.; Mu, Y.; Tian, Q.; et al. Selective Degeneration of Entorhinal-CA1 Synapses in Alzheimer's Disease via Activation of DAPK1. *J. Neurosci.* **2016**, *36*, 10843–10852. [Google Scholar] [CrossRef]
37. Yang, X.; Yao, C.; Tian, T.; Li, X.; Yan, H.; Wu, J.; Li, H.; Pei, L.; Liu, D.; Tian, Q.; et al. A novel mechanism of memory loss in Alzheimer's disease mice via the degeneration of entorhinal-CA1 synapses. *Mol. Psychiatry* **2018**, *23*, 199–210. [Google Scholar] [CrossRef]
38. Hadzibegovic, S.; Bontempi, B.; Nicole, O. Investigating the Impact of NMDA Receptor Organization and Biological Sex in the APPswe/PS1dE9 Mouse Model of Alzheimer's Disease. *Int. J. Mol. Sci.* **2025**, *26*, 1737. [Google Scholar] [CrossRef]
39. Berchtold, N.C.; Sabbagh, M.N.; Beach, T.G.; Kim, R.C.; Cribbs, D.H.; Cotman, C.W. Brain gene expression patterns differentiate mild cognitive impairment from normal aged and Alzheimer's disease. *Neurobiol. Aging* **2014**, *35*, 1961–1972. [Google Scholar] [CrossRef]
40. Meftah, S.; Gan, J. Alzheimer's disease as a synaptopathy: Evidence for dysfunction of synapses during disease progression. *Front. Synaptic Neurosci.* **2023**, *15*, 1129036. [Google Scholar] [CrossRef]
41. Subramanian, J.; Savage, J.C.; Tremblay, M.E. Synaptic Loss in Alzheimer's Disease: Mechanistic Insights Provided by Two-Photon in vivo Imaging of Transgenic Mouse Models. *Front. Cell Neurosci.* **2020**, *14*, 592607. [Google Scholar] [CrossRef]
42. Taddei, R.N.; Duff, K.E. Synapse vulnerability and resilience underlying Alzheimer's disease. *EBioMedicine* **2025**, *112*, 105557. [Google Scholar] [CrossRef]
43. Yu, S.P.; Jiang, M.Q.; Shim, S.S.; Pourkhodadad, S.; Wei, L. Extrasynaptic NMDA receptors in acute and chronic excitotoxicity: Implications for preventive treatments of ischemic stroke and late-onset Alzheimer's disease. *Mol. Neurodegener.* **2023**, *18*, 43. [Google Scholar] [CrossRef]
44. Jongsiriyanyong, S.; Limpawattana, P. Mild Cognitive Impairment in Clinical Practice: A Review Article. *Am. J. Alzheimers Dis. Other Demen* **2018**, *33*, 500–507. [Google Scholar] [CrossRef]
45. Filon, J.R.; Intorcia, A.J.; Sue, L.I.; Vazquez Arreola, E.; Wilson, J.; Davis, K.J.; Sabbagh, M.N.; Belden, C.M.; Caselli, R.J.; Adler, C.H.; et al. Gender Differences in Alzheimer Disease: Brain Atrophy, Histopathology Burden, and Cognition. *J. Neuropathol. Exp. Neurol.* **2016**, *75*, 748–754. [Google Scholar] [CrossRef]
46. Hohman, T.J.; Dumitrescu, L.; Barnes, L.L.; Thambisetty, M.; Beecham, G.; Kunkle, B.; Gifford, K.A.; Bush, W.S.; Chibnik, L.B.; Mukherjee, S.; et al. Sex-Specific Association of Apolipoprotein E With Cerebrospinal Fluid Levels of Tau. *JAMA Neurol.* **2018**, *75*, 989–998. [Google Scholar] [CrossRef]
47. Jack, C.R., Jr.; Wiste, H.J.; Weigand, S.D.; Knopman, D.S.; Vemuri, P.; Mielke, M.M.; Lowe, V.; Senjem, M.L.; Gunter, J.L.; Machulda, M.M.; et al. Age, Sex, and APOE epsilon4 Effects on Memory, Brain Structure, and beta-Amyloid Across the Adult Life Span. *JAMA Neurol.* **2015**, *72*, 511–519. [Google Scholar] [CrossRef]
48. Oveisgharan, S.; Arvanitakis, Z.; Yu, L.; Farfel, J.; Schneider, J.A.; Bennett, D.A. Sex differences in Alzheimer's disease and common neuropathologies of aging. *Acta Neuropathol.* **2018**, *136*, 887–900. [Google Scholar] [CrossRef]
49. Sundermann, E.E.; Biegon, A.; Rubin, L.H.; Lipton, R.B.; Mowrey, W.; Landau, S.; Maki, P.M.; Alzheimer's Disease Neuroimaging, I. Better verbal memory in women than men in MCI despite similar levels of hippocampal atrophy. *Neurology* **2016**, *86*, 1368–1376. [Google Scholar] [CrossRef]
50. Holland, D.; Desikan, R.S.; Dale, A.M.; McEvoy, L.K.; Alzheimer's Disease Neuroimaging, I. Higher rates of decline for women and apolipoprotein E epsilon4 carriers. *AJNR Am. J. Neuroradiol.* **2013**, *34*, 2287–2293, Erratum in *AJNR Am. J. Neuroradiol.* **2015**, *36*, E67. https://doi.org/10.3174/ajnr.A4545. [Google Scholar] [CrossRef]
51. Lin, K.A.; Choudhury, K.R.; Rathakrishnan, B.G.; Marks, D.M.; Petrella, J.R.; Doraiswamy, P.M.; Alzheimer's Disease Neuroimaging, I. Marked gender differences in progression of mild cognitive impairment over 8 years. *Alzheimers Dement* **2015**, *1*, 103–110. [Google Scholar] [CrossRef]

52. Buckley, R.F.; Mormino, E.C.; Rabin, J.S.; Hohman, T.J.; Landau, S.; Hanseeuw, B.J.; Jacobs, H.I.L.; Papp, K.V.; Amariglio, R.E.; Properzi, M.J.; et al. Sex Differences in the Association of Global Amyloid and Regional Tau Deposition Measured by Positron Emission Tomography in Clinically Normal Older Adults. *JAMA Neurol.* **2019**, *76*, 542–551. [Google Scholar] [CrossRef]
53. Coughlan, G.T.; Ourry, V.; Townsend, D.; Klinger, H.; Brown, J.A.; Cuppels, M.; Betthauser, T.; Langhough, R.; Cody, K.; Seto, M.; et al. Sex Differences in P-Tau217, Tau Aggregation, and Cognitive Decline. *JAMA Neurol.* **2026**, *83*, 369–381. [Google Scholar] [CrossRef]
54. Acosta-Martinez, M.; Carter, V.; Nessim, A.; Panchal, R.; John, D.; Dhawan, J.; Beach, T.G.; Serrano, G.E.; Sundermann, E.E.; Biegon, A. Sex- and region-dependent neuroinflammation in Alzheimer's disease. *Alzheimers Dement.* **2025**, *21*, e14603. [Google Scholar] [CrossRef]
55. Seto, M.; Clifton, M.; Gomez, M.L.; Coughlan, G.; Gifford, K.A.; Jefferson, A.L.; De Jager, P.L.; Bennett, D.A.; Wang, Y.; Barnes, L.L.; et al. Sex-specific associations of gene expression with Alzheimer's disease neuropathology and ante-mortem cognitive performance. *Nat. Commun.* **2025**, *16*, 9466. [Google Scholar] [CrossRef]
56. Digma, L.A.; Madsen, J.R.; Rissman, R.A.; Jacobs, D.M.; Brewer, J.B.; Banks, S.J.; Alzheimer's Disease Neuroimaging, I. Women can bear a bigger burden: Ante- and post-mortem evidence for reserve in the face of tau. *Brain Commun.* **2020**, *2*, fcaa025. [Google Scholar] [CrossRef]
57. Boccalini, C.; Peretti, D.E.; Scheffler, M.; Mu, L.; Griffa, A.; Testart, N.; Allali, G.; Prior, J.O.; Ashton, N.J.; Zetterberg, H.; et al. Sex differences in the association of Alzheimer's disease biomarkers and cognition in a multicenter memory clinic study. *Alzheimers Res. Ther.* **2025**, *17*, 46. [Google Scholar] [CrossRef]
58. Rossler, M.; Zarski, R.; Bohl, J.; Ohm, T.G. Stage-dependent and sector-specific neuronal loss in hippocampus during Alzheimer's disease. *Acta Neuropathol.* **2002**, *103*, 363–369. [Google Scholar] [CrossRef]
59. West, M.J.; Coleman, P.D.; Flood, D.G.; Troncoso, J.C. Differences in the pattern of hippocampal neuronal loss in normal ageing and Alzheimer's disease. *Lancet* **1994**, *344*, 769–772. [Google Scholar] [CrossRef]
60. Davolio, C.; Greenamyre, J.T. Selective vulnerability of the CA1 region of hippocampus to the indirect excitotoxic effects of malonic acid. *Neurosci. Lett.* **1995**, *192*, 29–32. [Google Scholar] [CrossRef]
61. Zhu, H.; Yoshimoto, T.; Imajo-Ohmi, S.; Dazortsava, M.; Mathivanan, A.; Yamashima, T. Why are hippocampal CA1 neurons vulnerable but motor cortex neurons resistant to transient ischemia? *J. Neurochem.* **2012**, *120*, 574–585. [Google Scholar] [CrossRef]
62. Stanika, R.I.; Winters, C.A.; Pivovarova, N.B.; Andrews, S.B. Differential NMDA receptor-dependent calcium loading and mitochondrial dysfunction in CA1 vs. CA3 hippocampal neurons. *Neurobiol. Dis.* **2010**, *37*, 403–411. [Google Scholar] [CrossRef]
63. Beach, T.G.; Adler, C.H.; Sue, L.I.; Serrano, G.; Shill, H.A.; Walker, D.G.; Lue, L.; Roher, A.E.; Dugger, B.N.; Maarouf, C.; et al. Arizona Study of Aging and Neurodegenerative Disorders and Brain and Body Donation Program. *Neuropathology* **2015**, *35*, 354–389. [Google Scholar] [CrossRef]
64. Biegon, A.; Fry, P.A.; Paden, C.M.; Alexandrovich, A.; Tsenter, J.; Shohami, E. Dynamic changes in N-methyl-D-aspartate receptors after closed head injury in mice: Implications for treatment of neurological and cognitive deficits. *Proc. Natl. Acad. Sci. USA* **2004**, *101*, 5117–5122. [Google Scholar] [CrossRef]
65. Marquie, M.; Normandin, M.D.; Vanderburg, C.R.; Costantino, I.M.; Bien, E.A.; Rycyna, L.G.; Klunk, W.E.; Mathis, C.A.; Ikonomovic, M.D.; Debnath, M.L.; et al. Validating novel tau positron emission tomography tracer [F-18]-AV-1451 (T807) on postmortem brain tissue. *Ann. Neurol.* **2015**, *78*, 787–800. [Google Scholar] [CrossRef]
66. Duvernoy, H.; Cattin, F.; Risold, P.-Y. *The Human Hippocampus: Functional Anatomy, Vascularization and Serial Sections with MRI*, 4th ed.; Springer: New York, NY, USA, 2013. [Google Scholar]

Disclaimer/Publisher's Note: The statements, opinions and data contained in all publications are solely those of the individual author(s) and contributor(s) and not of MDPI and/or the editor(s). MDPI and/or the editor(s) disclaim responsibility for any injury to people or property resulting from any ideas, methods, instructions or products referred to in the content.